Spectrochimica Acta Part A 79 (2011) 1375–1380

Contents lists available at ScienceDirect

Spectrochimica Acta Part A: Molecular and Biomolecular Spectroscopy

journal homepage: www.elsevier.com/locate/saa

Investigation into the regiochemistry of some isoxazoles derived from 1,3-dipolar cycloaddition of 4-nitrobenzonitrile oxide with some dipolarophiles: A combined theoretical and experimental studies

N. Dorostkar-Ahmadi[a], M. Bakavoli[a,*], F. Moeinpour[b], A. Davoodnia[a]

[a] *Department of Chemistry, Faculty of Science, Islamic Azad University, Mashhad Branch, Mashhad, Iran*
[b] *Department of Chemistry, Faculty of Science, Islamic Azad University, Bandar Abbas Branch, Bandar Abbas, Iran*

ARTICLE INFO

Article history:
Received 4 November 2010
Received in revised form 16 April 2011
Accepted 29 April 2011

Keywords:
Regioselectivity
1,3-dipolar cycloaddition
Nitrile oxide
DFT-based reactivity indexes
B3LYP calculations

ABSTRACT

Reaction of 4-nitrobenzonitrile oxide(2) which was generated in situ with acrylo nitrile (3), methyl methacrylate (4) and allyl bromide (5) as dipolarphile afforded the new 7a, 8a and 9a compounds respectively. Reactivity and regiochemistry of these reactions were investigated using activation energy calculations and density functional theory (DFT)-based reactivity indexes. The theoretical ^{13}C NMR chemical shifts of the cycloadducts which were obtained by GIAO method were comparable with the observed values.

1. Introduction

The cycloaddition of 1,3-dipolar species to an alkene for the synthesis of five-membered rings is a classic and important reaction in organic chemistry [1]. These 1,3-dipolar cycloaddition (1,3-DC) reactions are used for both academia and industrial purposes [2]. These reactions are one of the most important processes with both synthetic and mechanistic interest in organic chemistry. Current understanding of the underlying principles in the Diels–Alder (DA) reactions and the 1,3-dipolar cycloadditions (1,3-DC) has grown from a fruitful interplay between theory and experiment [2–4]. The stereochemistry of these reactions may be controlled either by choosing the appropriate substrates or by controlling the reaction using a metal complex acting as catalyst [5].

The 1,3-DC reactions possess several interesting characteristics, in particular, regioselectivity. Fleming [6] demonstrated that the Frontier molecular orbital model (FMO) seems to be able to explain the observed regioselectivity and reactivity differences. Although transition state theory remains the most widely used and the most rigorous approach for the study of the mechanism and the regiochemistry of these reactions, the localization of transition states is not always easier.

Furthermore, transition-state calculations are often very time consuming when bulky substitutents are present in reactive systems. The nature of the 1,3-DC reactions is still an open arena in physical organic chemistry. So many studies have been carried out for these reactions [7–9].

Recently, reactivity descriptors based on the density functional theory (DFT), such as Fukui indexes, local softnesses and local electrophilicity, have been extensively used for the prediction of the regioselectivity. For instance, several treatments of 1, 3-DC reactions of nitrile oxides with various dipolarophiles can be found in the literature [10–15]. In this context, we became interested in the reactivity of nitrile oxide (2) as dipole towards acrylonitrile (3), methyl methacrylate (4) and allyl bromide (5) as dipolarophiles in order to synthesize the new 3-(4-nitrophenyl)-4,5-dihydroisoxazole-5-carbonitrile (6a), methyl 5-methyl-3-(4-nitrophenyl)-4,5-dihydroisoxazole-5-carboxylate(7a) and 4-(bromomethyl)-3-(4-nitrophenyl)-4,5-dihydroisoxazole (8a) (Fig. 1). In addition, we found it worthwhile to analyze the regioselectivity of these 1,3-DC reactions by several theoretical approaches, namely, activation energy calculations and DFT-based reactivity indexes. Finally, the gauge-invariant atomic orbital (GIAO) method [16] was used to calculate NMR chemical shifts, to help the experimental cycloadduct determination, because it has shown to yield data comparable to those of the experiment [17].

2. Regioselectivity criteria for two-center reactions

A useful simplification for the study of the regioselectivity in reactions may be obtained by looking at those processes

---

* Corresponding author. Tel.: +98 511 879 7022; fax: +98 511 879 6416.
E-mail address: mbakavoli@yahoo.com (M. Bakavoli).

1386-1425/$ – see front matter © 2011 Elsevier B.V. All rights reserved.
doi:10.1016/j.saa.2011.04.071

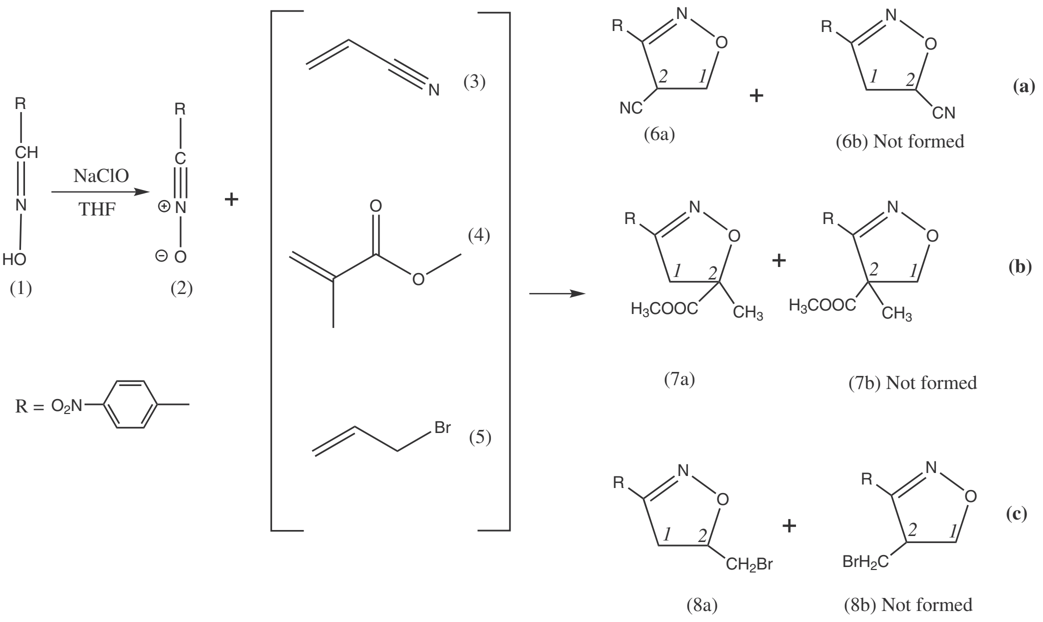

Fig. 1. The regioisomeric pathways for 1,3-DC of benzonitrile oxide (2) and dipolarophiles (3), (4) and (5).

having a markedly polar character, where the transition structure associated with the rate-determining step mostly involves the formation of one single bond between the most electrophilic and other nucleophilic sites. According to the model recently proposed by Domingo [18,19], during an electrophile–nucleophile interaction process, The preferred interaction will be through the most electrophilic site of the former and the most nucleophilic site of the latter. Local philicity indexes (for definition, see computational details) are therefore expected to be useful descriptor of regional electrophilicity/nucleophilicity patterns that may account for the observed regioselectivity in two-center reactions with a significant polar character.

3. Computational methods

All calculations were performed with the Gaussian98 program suite [20]. For DFT calculations, the B3LYP/6-31G (d) level of theory was employed. The optimizations of equilibrium geometries of reactants and products were performed using the Berny analytical gradient optimization method [21]. The transition states (TSs) for the 1,3-DC reactions have been localized at the B3LYP/6-31G (d) level of theory. The stationary points were characterized by frequency calculations in order to verify that the TSs had one and only one imaginary frequency.

The global electrophilicity for dipole and dipolarophile was evaluated using Eq. (1) [22]:

$$\omega = \frac{\mu^2}{2\eta} \qquad (1)$$

In Eq. (1) μ and η are the electronic chemical potential and the chemical hardness of the ground state (GS) of atoms and molecules, respectively.

The electronic chemical potential μ and chemical hardness η were evaluated in terms of the one electron energies of the FMOs, HOMO and LUMO, using Eqs. (2) and (3), respectively [23,24]:

$$\mu \approx \frac{\varepsilon_H + \varepsilon_L}{2} \qquad (2)$$

$$\eta \approx (\varepsilon_H - \varepsilon_H) \qquad (3)$$

As usual, local indexes are computed in atomic condensed form [25]. The well-known Fukui function [26] for electrophilic (f_k^-) and nucleophilic attack (f_k^+) have been evaluated from single point calculations performed at the GS of molecules at the same level of theory, using a method described elsewhere [27]. This method evaluates the Fukui functions using the coefficients of the frontier molecular orbitals involved in the reaction and the overlap matrix.

The local electrophilicity index, ω_k, condensed to atom k is easily obtained by projecting the global quantity onto any atomic center k in the molecule by using the electrophilic Fukui function (i.e. the Fukui function for nucleophilic attack, f_k^+ [28])

$$\omega_k = \omega f_k^+ \qquad (4)$$

Recently, Domingo et al. has introduced an empirical (relative) nucleophilicity index [29], N, based on the HOMO energies obtained within the Kohn–Sham scheme, [24] and defined as E_{HOMO}(Nu)–E_{HOMO}(TCE). This nucleophilicity scale is referred to tetracyanoethylene (TCE) taken as a reference.

Local nucleophilicity [30] index, N_k, was evaluated using the following equation:

$$N_k = N f_k^- \qquad (5)$$

where f_k^- is the Fukui function for an electrophilic attack [26].

The ^{13}C NMR chemical shifts were calculated by means of the GIAO method [16], using the tetramethylsilane (TMS) as ^{13}C reference, at the B3LYP/6-31G (d)level of theory (reference value of ^{13}C = 184(5307 ppm).

4. Experimental

The melting points were recorded on an Electrothermal type 9100 melting point apparatus. The ^{1}H NMR (400 MHz) spectra were recorded on a Bruker AC 400 spectrometer. ^{13}C NMR spectra were determined using the Bruker AM-400 instrument operating at 100 MHz. IR spectra were determined as KBr pellets on a Bruker model 470 spectrophotometer. The mass spectra were scanned on a Varian Mat CH-7 instrument at 70 eV. Elemental analyses were carried out on Carlo Erba CHNS-O 1108 apparatus and were in good accordance with theoretical data. Oxime (1) the precursor of nitrile oxide (2) is a known compound was prepared according to generally used methods [31] (for characterization data of newly prepared compounds, see Table 1 and for spectral data, see Table 2).

Table 1
Characterization data of newly prepared compounds 6a, 7a, and 8a.

Compound	Formula	M_r	w_i(calc.)/% w_i(found)/%			Yield	M.p.
			C	H	N	%	°C
6a	$C_{10}H_7N_3O_3$	217	55.30	3.25	19.35	81	161–163
			55.84	3.87	19.05		
7a	$C_{12}H_{12}N_2O_5$	264	54.55	4.58	10.60	88	130–132
			54.55	4.63	10.56		
8a	$C_{10}H_9BrN_2O_3$	285	42.13	3.18	9.83	85	166–168
			42.04	3.24	9.86		

4.1. General procedure for the synthesis of cycloadducts

To a mixture of 1 mmol of oxime and 1.5 mmol of dipolarophile in tetrahydrofuran (THF) (25 mL) was added aqueous NaOCl (11% Cl_2 content, 1.62 mL, 2.50 mmol) at 5 °C. The reaction was stirred for 10 min, then at r.t. for 24 h. After that, H_2O (30 mL) was added, the organic layer separated and remaining product extracted from the aqueous layer using $CHCl_3$ (15 mL). The combined organic layers were washed with H_2O (20 mL), dried (Na_2SO4) and the solvent was removed under reduced pressure. The crude product was purified by precipitation with cold Et_2O to afford cycloadducts as yellow crystals.

5. Results and discussion

Nitrile oxide (2) was generated in situ from the oxime (1) in a mixture of aqueous NaClO in THF. 1,3-DC of nitrile oxide (2) with the dipolarophiles proceeded smoothly in a selective manner to give a single regioisomer of each pair 6a-b, 7a-b, and 8a-b in very good yields (Fig. 1). It should be noted that the absence of the nitrile absorption band in the IR spectrum of the cycloadduct 6a, is the reminiscent of the previously reported observations with the aliphatic nitriles which are activated by a nitrogen or an oxygen atom in their β-position [32–34]. The assignment of the regiochemistry of these products was based upon (*i*) comparing the theoretical ^{13}C NMR spectral data obtained by GIAO method with the observed values for both regioisomers; (*ii*) activation energy calculations and (iii) DFT-based reactivity indexes.

Table 3
The comparison of theoretical ^{13}C NMR chemical shifts data (Δ, ppm) of C-1 and C-2 of each pair of regioisomers with those obtained from the experimental ^{13}C NMR spectroscopy.

Compound	Atom number	Calculated chemical shift	Experimental chemical shift
6a	C-1	41.3	40.6
	C-2	68.5	67.3
6b	C-1	56.4	
	C-2	21.3	
7a	C-1	44.6	44.1
	C-2	90.8	87.3
7b	C-1	64.5	
	C-2	39.9	
8a	C-1	79.7	80.6
	C-2	39.4	39.0
8b	C-1	35.1	
	C-2	72.6	

(*i*) For further cycloadduct characterization, we obtained the theoretical ^{13}C chemical shifts values for the products through the GIAO method and compared it with the observed values. As it can be seen in Table 3, the observed values for C1 and C2 in each of the isolated products (40.6, 67.3;44.1, 87.3 and 80.6,39.0 ppm in compounds 6, 7 and 8 respectively) are in close proximity to the theoretical values for compounds 6a, 7a, and 8a. It seems likely that the isolated regioisomers are structurally similar to 6a, 7a and

Table 2
Spectral data of newly prepared compounds 6a, 7a and 8a.

Compound	Spectral data
6a	IR, $\tilde{\nu}$/cm^{-1}: 1599 (C=N), 1515 $(NO_2)_{as}$, 1347 $(NO_2)_s$ ^{1}H NMR ($CDCl_3$), δ/ppm: 3.79(1H, dd, CH_AH_B, J = 6.80 Hz, J = 10.0 Hz), 3.86 (1H, dd, CH_AH_B, J = 6.00 Hz, J = 11.20 Hz), 5.56 (1H, dd, CH, J = 6.40 Hz, J = 6.80 Hz), 7.88 (2H, d, CH–Ar, J = 9.60 Hz), 8.34 (2H, d, CH–Ar, J = 8.80 Hz) ^{13}C NMR ($CDCl_3$), δ/ppm: 40.6 (CH_2), 67.3(CH), 116.5 (C≡N), 124.3, 128.0, 133.3, 149.2 (C_{Ph}), 154.8 (C=N) MS, m/z: 217 (M^+)
7a	IR, $\tilde{\nu}$/cm^{-1}: 1728(C=O), 1599(C=N), 1513 $(NO_2)_{as}$, 1347 $(NO_2)_s$ ^{1}H NMR ($CDCl_3$), δ/ppm: 1.77 (3H, s, CH_3), 3.27 (1H, d, CH_AH_B, J = 17.20 Hz), 3.84 (3H, s, OCH_3), 3.95 (1H, d, CH_AH_B, J = 16.80 Hz), 7.84 (2H, d, CH–Ar, J = 8.80 Hz), 8.28 (2H, d, CH–Ar, J = 8.80 Hz). ^{13}C NMR ($CDCl_3$), δ/ppm: 23.6 (CH_3), 44.1 (CH_2), 53.2 (OCH_3), 87.3 (C), 124.0, 127.5, 135.1, 148.6, 154.8 (C=N), 172.0 (C=O) MS, m/z: 264 (M^+)
8a	IR, $\tilde{\nu}$/cm^{-1}: 1607 (C=N), 1518 $(NO_2)_{as}$, 1350 $(NO_2)_s$ ^{1}H NMR ($CDCl_3$), δ/ppm: 3.39 (1H, dd, CH_AH_B, J = 6.40 Hz, J = 10.40 Hz), 3.49 1H, dd, CH_AH_B, J = 8.00 Hz, J = 2.40 Hz), 3.57 (1H, dd, CH_AH_B, J = 6.00 Hz, J = 10.80 Hz), 3.64 (1H, dd, CH_AH_B, J = 4.00 Hz, J = 6.80 Hz), 5.20 (1H, m, CH), 7.87 (2H, d, CH–Ar, J = 8.80 Hz), 8.30 (2H, d, CH–Ar, J = 8.80 Hz). ^{13}C NMR ($CDCl_3$), δ/ppm: 32.9 (CH_2Br), 39.0 (CH), 80.6 (CH_2), 124.1, 127.5, 135.1, 148.7 (C_{Ph}), 154.6 (C=N). MS, m/z: 284 (M^+), 286 (M^++2).

Table 4
Energies of reactives, transition states and cycloadducts 6, 7 and 8, E (a.u.), relative activation energies ΔE_a (kcal mol^{-1}) and relative energies between products and reactives, ΔE_r (kcal mol^{-1}).

	E	ΔE_a*	ΔE_r*
Reaction a			
Nitrilie oxide 2	−604.1384		
Acrylonitrile 3	−170.8316		
TS 6a	−774.9500	12.5	
TS 6b	−774.9485	13.5	
6a	−775.0274		−36.0
6b	−775.0259		−35.1
Reaction b			
Nitrilie oxide 2	−604.1384		
Methyl methacrylate 4	−345.7980		
TS 7a	−949.9068	18.6	
TS 7b	−949.8991	23.4	
7a	−949.9877		−32.2
7b	−949.9768		−25.3
Reaction c			
Nitrilie oxide 2	−604.1384		
Allyl bromide 5	−2689.0054		
TS 8a	−3293.1311	7.9	
TS 8b	−3293.1262	11.0	
8a	−3293.2201		−47.9
8b	−3293.2137		−43.9

* To reactives.

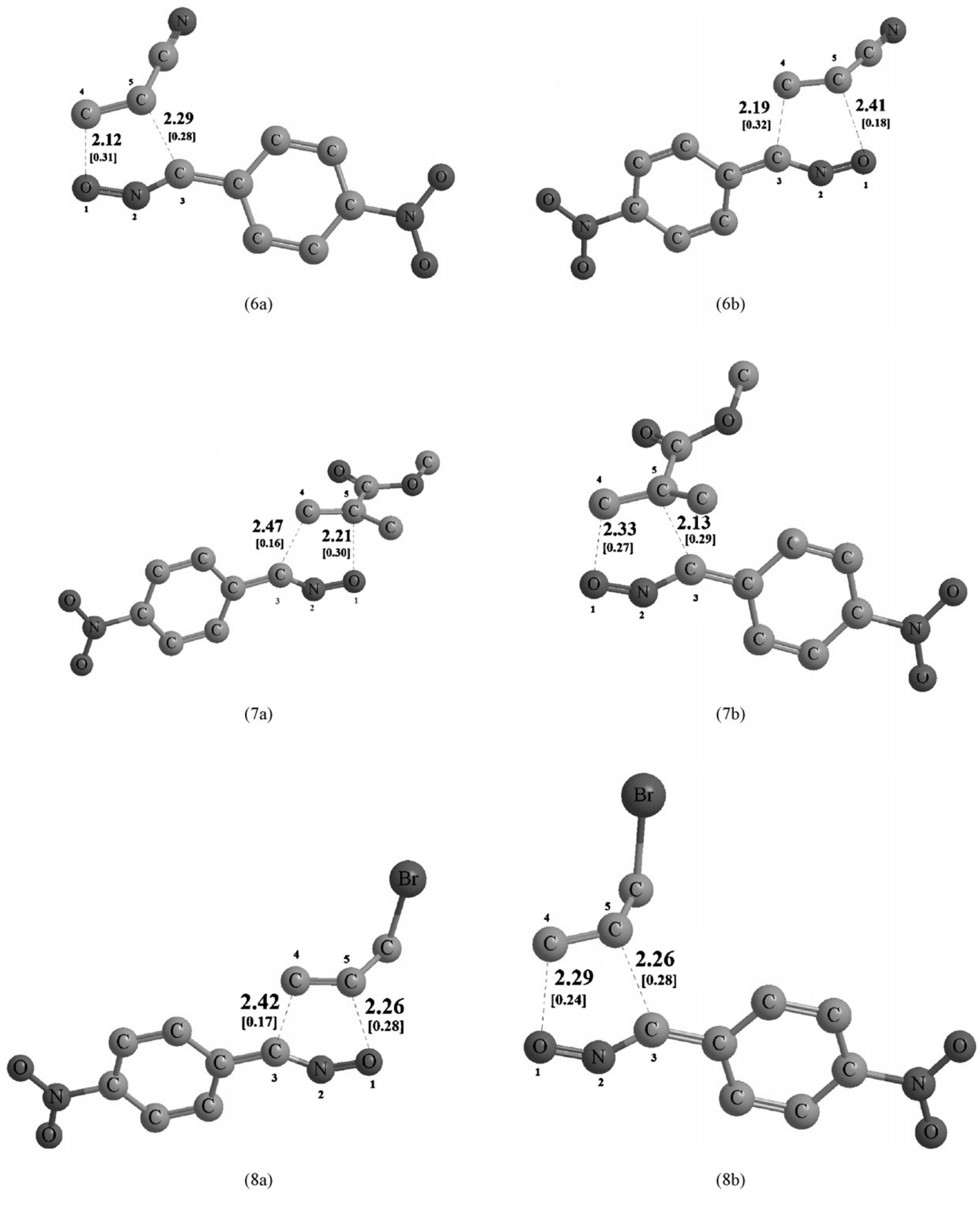

(6a) (6b)

(7a) (7b)

(8a) (8b)

Fig. 2. Optimized geometries for transition state structures at the B3LYP/6-31G (d) level of theory. Hydrogen atoms have been omitted for clarity. Distances of forming bonds are given in angstroms. The bond orders are given in brackets.

Table 5
HOMO, LUMO energies in a.u., electronic chemical potential (μ in a.u.), chemical hardness (η, in a.u.), global electrophilicity (ω, in eV) and global nucleophilicity (N, in eV) for dipole and dipolarophile systems.

	HOMO	LUMO	μ	η	ω	N[a]
Dipole(nitrile oxide)	−0.259	−0.111	−0.185	0.148	3.15	2.07
Dipolarophil(acrylonitrile)	−0.289	−0.056	−0.173	0.233	1.74	1.25
Dipolarophile (methyl methacrylate)	−0.268	−0.039	−0.153	0.229	1.39	1.84
Dipolarophile (allyl bromide)	−0.264	−0.004	−0.134	0.260	0.93	1.94

[a] The HOMO energy of tetracyanoethylene is −0.3351 a.u. at the same level of theory.

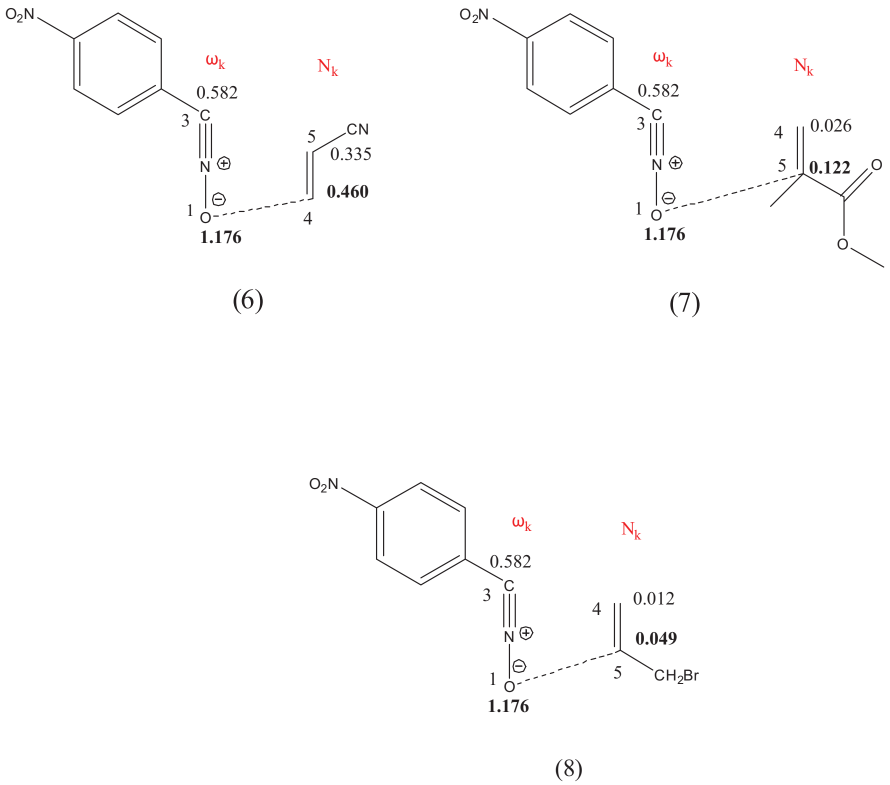

Fig. 3. Illustration of the favorable interactions using Local nucleophilicities, N_k, for dipolaropile centers and local electrophilicities, ω_k, for the nitril oxide centers.

8a. Further proofs came from activation energy and DFT studies as followings:

(*ii*) Activation energy calculations: The transition states have been localized for both cyclization modes. The corresponding activation energies and structures are given in Table 4 and Fig. 2 respectively. An analysis of the geometries at the TSs given in Fig. 2 indicates that they correspond to an asynchronous bond formation processes. The extent of bond formation along a reaction pathway is provided by the concept of bond order (BO) [35]. The BO (Wiberg indexes) values of the O–C and C–C forming bonds at TSs are shown in brackets in Fig. 2. These values are within the range of 0.16–0.32. Therefore, it may be suggested that these TSs correspond to early processes. In general, the asynchronicity shown by the geometrical data is accounted for by the BO values. A qualitative reactivity can be estimated by applying Hammond's postulate [36]. All of the reactions proceeded exothermically with large ΔE_r (relative energies between products and reactives) energy values. According to Hammond's postulate, the TSs should then be closer to the reactives. The activation energy values, ΔE_a, also favor the formation of the cycloadducts 6a, 7a, and 8a against their regioisomers 6b, 7b, and 8b respectively.

(*iii*) DFT-based reactivity indexes: Prediction of regiochemistry by using DFT-based reactivity indexes. The chemical hardnesses η, global electrophilicity ω and global nucleophilicity N of the nitrile oxide and dipolarophiles are given in Table 5. The Fukui indexes for the atoms O1 and C3 of the dipole (nitrile oxide) and for the atoms C4 and C5 of the dipolarophiles (acrylonitrile, methyl methacrylate and allyl bromide) are given in Table 6 (see Fig. 3 for atom numbering).

As it can be seen in Table 5, the electronic chemical potential of dipolarophiles acrylonitrile, methyl methacrylate and allyl bromide is greater than that of nitrile oxide (dipole), which indicates the charge transfer is taking place from dipolarophiles to nitrile oxide. Note that even though nitrile oxide (dipole) has a larger electrophilicity (ω) and nucleophilicity (N) values than dipolarophiles, it has a lower chemical potential, which is the index that determines the direction of the electronic flux along the cycloaddition [37]. In Fig. 3, we have reported the values of local electrophilicities ω_k for atoms O1 and C3 of the dipole (nitrile oxide) and the local nucleophilicities N_k for atoms C4 and C5 of dipolarophiles in 6, 7 and 8. According to the Domingo's model [29,30], the local philicity indexes (ω_k, N_k) seem to be a reliable tool for the prediction of the most favored interaction in a two-center polar process. It turns out that the two-center polar model, based on electrostatic charges, predicts correctly the experimental regioselectivity [29,30].

Table 6

Fukui indexes for the O1 and C3 atoms of the nitrile oxide and for atoms C4 and C5 of the dipolarophiles.

	Atom number	f_k^+	f_k^-
Nitrile oxide	O1	0.373	
	C3	0.185	
Acrylonitrile	C4		0.368
	C5		0.268
Methyl methacrylate	C4		0.014
	C5		0.066
Allyl bromide	C4		0.006
	C5		0.025

6. Conclusions

The regioselectivity for the 1,3-DC reactions of nitrile oxide (2) with acrylonitrile(3), methyl methacrylate (4) and allyl bromide (5) has been investigated using experimental and theoretical ^{13}CNMR studies together with the activation energy calculations and the DFT-based reactivity indexes at the B3LYP/6-31G(d) level of theory. The results obtained in this work clearly predict the regiochemistry of the isolated cycloadducts.

References

[1] K.V. Gothelf, K.A. Jorgensen, Chem. Rev. 98 (1998) 863.
[2] A. Padwa, 1,3-Dipolar Cycloaddition Chemistry, Wiley/Interscience, New York, 1984.
[3] A. Wasserman, Diels–Alder Reactions, Elsevier, NewYork, 1965.
[4] I. Fleming, Pericyclic Reactions, Oxford University, Oxford, 1999.
[5] K.V. Gothelf, Asymmetric Metal-Catalysed 1,3-Dipolar Cycloaddition Reactions, Wiley/VCH, Weinheim, New York, 2001.
[6] I. Fleming, Frontiers Orbitals and Organic Chemical Reactions, Wiley, London, 1976.
[7] W. Benchouk, S.M. Mekelleche, J. Mol. Struct. (Theochem.) 852 (2008) 46.
[8] F. Moeinpour, Chin. J. Chem. Phys. 23 (2010) 165.
[9] M. Bakavoli, F. Moeinpour, A. Davoodnia, A. Morsali, J. Mol. Struct. 969 (2010) 139.
[10] K.H. Kang, A.N. Pae, K.I. Choi, Y.S. Cho, B.Y. Chung, J.E. Lee, S.H. Jung, H.Y. Koh, H.Y. Lee, Tetrahedron Lett. 42 (2001) 1057.
[11] Y.J. Shang, Y.G. Wang, Synthesis (2002) 1663.
[12] B.B. Shankar, D.Y. Yang, S. Girton, A.K. Ganguly, Tetrahedron Lett. 39 (1998) 2447.
[13] R.S. Kumar, S.M. Rajesh, S. Perumal, P. Yogeeswari, D. Sriram, Tetrahedron Asymm. 21 (2010) 1315.
[14] S. Chen, J. Ren, Z. Wang, Tetrahedron 65 (2009) 9146.
[15] A.K. Nacereddine, W. Yahia, S. Bouacha, A. Djerourou, Tetrahedron Lett. 51 (2010) 2617.
[16] K. Wolinski, J.F. Hilton, P. Pulay, J. Am. Chem. Soc. 112 (1990) 8251.
[17] A. Garcĭıa-Granados, E. Melguizo, A. Parra, J. Org. Chem. 65 (2000) 8214.
[18] L.R. Domingo, M.J. Aurell, P. Pérez, R. Contreras, Tetrahedron 58 (2002) 4417.
[19] P. Pérez, L.R. Domingo, M.J. Aurell, R. Contreras, Tetrahedron 59 (2003) 3117.
[20] M.J. Frisch, et al., Gaussian 98, Revision A.7, Gaussian Inc., Pittsburgh PA, 1998.
[21] H.B. Schlegel, J. Comput. Chem. 3 (1982) 214.
[22] R.G. Parr, L.V. Szentpály, S. Liu, J. Am. Chem. Soc. 121 (1999) 1922.
[23] R.G. Parr, W. Yang, Density Functional Theory of Atoms and Molecules, Oxford University Press, New York, 1989.
[24] R.G. Parr, R.G. Pearson, J. Am. Chem. Soc. 105 (1983) 7512.
[25] W. Yang, W.J. Mortier, J. Am. Chem. Soc. 108 (1986) 5708.
[26] K. Fukui, Science 218 (1982) 747.
[27] R. Contreras, P. Fuentealba, M. Galván, P. Pérez, Chem. Phys. Lett. 304 (1999) 405.
[28] L.R. Domingo, M.J. Aurell, P. Pérez, J. Phys. Chem. A 106 (2002) 6871.
[29] L.R. Domingo, P. Pérez, J. Org. Chem. 73 (2008) 4615.
[30] P. Pérez, L.R. Domingo, M. Duque-Noreña, E. Chamorro, J. Mol. Struct. (Theochem.) 895 (2009) 86.
[31] A. Schoffstall, B. Gaddis, M. Druelinger, Microscale and Miniscale Organic Chemistry Laboratory Experiments, Mc Graw Hill Inc., London, 2004.
[32] J.P. Jesson, H.W. Thompson, Spectrochim. Acta 13 (1958) 217.
[33] G. Butt, J. Cilmi, P.M. Hooben, R.D. Topsom, Spectrochim. Acta: Mol. Spectrosc. 36A (1980) 521.
[34] N.M. Abunada, H.M. Hassaneen, N.G. Kandile, O.A. Miqdad, Molecules 13 (2008) 1011.
[35] K.B. Wiberg, Tetrahedron 24 (1968) 1083.
[36] G.S. Hammond, J. Am. Chem. Soc. 77 (1955) 334.
[37] M.J. Aurell, L.R. Domingo, P. Perez, R. Contreras, Tetrahedron 60 (2004) 11503.